19th Brazilian Congress of Thermal Sciences and Engineering
November 06th-10th, 2022, Bento Gonçalves - RS - Brazil

ENC-2022-0670
ASSESSMENT OF DESALINATION VIA MEMBRANE DISTILLATION USING LOW-GRADE WASTE HEAT IN SMALL MODULAR REACTORS

Gabriel C. G. R. da Silva
Nuclear Engineering Program, Federal University of Rio de Janeiro, COPPE/UFRJ, Rio de Janeiro, RJ, Brazil
gabriel.caetano@coppe.ufrj.br

Kleber Marques Lisbôa
Department of Mechanical Engineering, Fluminense Federal University, UFF, Niterói, RJ, Brazil
kmlisboa@id.uff.br

Jian Su
Nuclear Engineering Program, Federal University of Rio de Janeiro, COPPE/UFRJ, Rio de Janeiro, RJ, Brazil
sujian@coppe.ufrj.br

Carolina P. Naveira-Cotta
Mechanical Engineering Program, Federal University of Rio de Janeiro, COPPE/UFRJ, Rio de Janeiro, RJ, Brazil
carolina@mecanica.coppe.ufrj.br

Renato M. Cotta
Mechanical Engineering Program, Federal University of Rio de Janeiro, POLI&COPPE/UFRJ, Rio de Janeiro, RJ, Brazil
IPqM/ DGDNTM, General Directorate of Nuclear and Technological Development, Brazilian Navy, Rio de Janeiro, RJ, Brazil
cotta@mecanica.coppe.ufrj.br

Abstract. *Membrane distillation has been gaining recognition as an alternative desalination method, with a niche in processing high salinity brines and using low-grade heat sources. In the present analysis, membrane distillation was estimated to produce 2,012.1 m³/day of distilled water using solely the waste heat from the turbine exhaust of NuScale, a well-known small modular reactor (SMR) design. The heat recovery unit was shown to be fundamental for improving the efficiency of the desalination system. When the recovery heat exchangers have an effectiveness of 0.9, the gain-output ratio (GOR), used to assess the desalination efficiency, increased nearly fourfold compared to the system without heat recovery. Results showed that the ratio between the feed and the permeate flow rates presented an optimum value of 2.1 for the studied configuration.*

Keywords: *Nuclear desalination, Membrane distillation, Waste heat recovery, Cogeneration, SMR, DCMD*

1. INTRODUCTION

In order to cope with the world's increasing water scarcity, desalination techniques are expected to play a leading role within the upcoming decades (Voutchkov, 2018). Since water desalination is a highly energy-intensive process, it is common to find desalination facilities thermodynamically coupled to nuclear power plants (Mantero et al., 2014; Alonso et al., 2012), providing cogeneration by recovering part of the reactor's useful and/or waste heat for desalination. Among the existing water desalination technologies, the most employed are the multi-stage flash (MSF), multi-effect distillation (MED), and reverse osmosis (RO). MSF and MED are based on thermal processes and consume more total energy, but produce a higher quality product, whereas RO is a membrane technique and demands much less energy per unit mass of product but employs electricity and produces water still with a certain concentration of salts (Alonso et al., 2012).

With the intent of combining the advantages of both thermal and membrane processes, the membrane distillation (MD) technology was proposed by Findley (1967). It consists of a membrane separation process based on the partial pressure gradient across a hydrophobic membrane. This pressure gradient occurs because of the temperature difference between the hot saline feed water and the cold permeate solution. This technology enables the reuse of low-grade waste heat, which means, it allows the production of additional distilled water from waste heat without deducting from the power generated by the plant, and the product has a superior quality compared to RO (Deshmukh et al., 2018).

The Brazilian domestic development of a small modular pressurized water reactor (PWR) for cogeneration of water and electricity could improve the capacity of the nation to address the problem of water scarcity. Thus, in 2016, the DESSAL Project was launched by the National Commission of Nuclear Energy (CNEN), in collaboration with its research institutes, partner universities, and the Brazilian Navy, with the objective of proposing a new modular reactor, having the LABGENE project (land-based prototype of Brazil's first conventional submarine with nuclear propulsion) as a starting point, optimized for cogeneration of water and electricity. The DEEP (Desalination Economic Evaluation Program) code of the International Atomic Energy Agency (IAEA, 2013) was employed to evaluate the performance and costs of different configurations of cogeneration of electricity and desalinated water (Cotta et al., 2019). Preliminary analyses of the desalination capacity of a LABGENE-based SMR, with a compact core generating a thermal power of 75 MWt and reference electric power of 24 MWe, was evaluated using different hybrid configurations of desalination systems, in particular combining reverse osmosis (RO) and distillation (MED or MSF). For instance, the DEEP simulation for the case of reverse osmosis (RO) combined with multi-effect distillation (MED) for seawater desalination (salinity of 35,000 ppm), using 18 MWe of available electric power and a portion of heat recovered in the secondary circuit, resulted in a total production of about 132,000 m³/day of water with low average salinity (190 ppm) (Cotta et al., 2019). It should be noted that the software DEEP does not include the analysis of membrane distillation processes, which could still be explored via low-grade waste heat recovery in the secondary loop, enabling, for example, the extraction of distilled water from the reverse osmosis effluent brine, therefore increasing the water recovery factor of the plant.

Accurate prediction of membrane distillation performance in water desalination of direct contact membrane distillation (DCMD) with hollow-fiber membrane modules was accomplished in Lisboa et al. (2019). A single-fiber model was proposed and the efficiency of the desalination process was assessed. The membrane distillation process was recently further studied to investigate the relative importance of five different membrane parameters and their combinations on the energy efficiency of a desalination system employing a direct contact membrane distillation (DCMD) module and a heat recovery system (Lisboa et al., 2021). A porous medium model for the hollow-fiber membrane module was proposed and results showed that, in addition to improved membranes development, better designed heat recovery systems can lead to substantial energy efficiency enhancement in the MD process. Also quite recently, Sampaio (2022) studied the cogeneration via MD using the waste heat of a hypothetical power plant and concluded that there is a trade-off between the distillate flux and the thermal efficiency as the length of the module increases.

The present work investigates a possible thermal coupling design of the small modular reactor NuScale, which is one of the world's most advanced SMR projects, producing an electric power of 50 MWe per module (NuScale Power LLC, 2020), with a direct contact membrane distillation (DCMD) desalination plant using solely the waste heat rejected by the reactor secondary circuit. The aim is to estimate the bottom line in terms of distilled water, that can be produced with the simplest DCMD configuration and recovering just the low-grade waste heat from the turbine exhaust before going into the condenser, using the minimum electricity, only for the additional pumping required by the desalination system with heat recovery.

2. METHODOLOGY

The proposed desalination plant flow diagram comprises three feed water pre-heaters, as shown in Fig. 1. Two of them are set to recover part of the heat from the MD module outlet streams, and the third one is where the exhaust steam from the turbine condenses, increasing the feed water temperature up to the MD module entrance temperature ($T_{e,s}$). This configuration is similar to the one proposed by Dutta et al. (2020). The second heat exchanger is set to operate only if the feed leaves the MD module at a higher temperature compared to the seawater feed after Heat Exchanger 1. If the temperature of the seawater feed after Heat Exchanger 1 surpasses the temperature of the feed module outlet, the second exchanger is not used since it would result in cooling of the feed instead of the desired pre-heating.

The membrane distillation module consists of a set of hollow fiber permeators working in parallel. The hot feed solution (saline water) in the shell side and the cold permeate (water at ambient temperature) in the lumen side (inside the hollow fiber) flow in countercurrent configuration. Using the Dusty Gas Model, the integrated equation for the distillate water flux through the membrane, at the lumen inner face, is given by Lisboa et al. (2021):

$$j_{w,l} = \frac{M_w D_{wa}^0}{R T_m r_l \ln(r_s/r_l)} \ln\left(\frac{D_{wa}^0 - D_{eff}\, p_s}{D_{wa}^0 - D_{eff}\, p_l}\right) \quad (1)$$

where M_w is the molar mass of water, p_s and p_l are the partial pressures at the membrane interface of the shell and lumen sides, respectively, D_{wa}^0 and D_{eff} are the ordinary and effective diffusivities, given by:

$$D_{wa}^0 = 4.46 \times 10^{-6} {\varepsilon_m}^2\, {T_m}^{2.334} \quad (2)$$

$$D_{eff} = \frac{D_w^k D_{wa}^0}{D_{wa}^0 + P D_w^k} \quad (3)$$

where ε_m and T_m are the membrane porosity and its average temperature, respectively. P is the total pressure within the pore and D_w^k is the Knudsen diffusivity, defined as:

$$D_w^k = \frac{{\varepsilon_m}^2 d_p}{3} \sqrt{\frac{8RT_m}{\pi M_w}} \tag{4}$$

where d_p is the pore diameter.

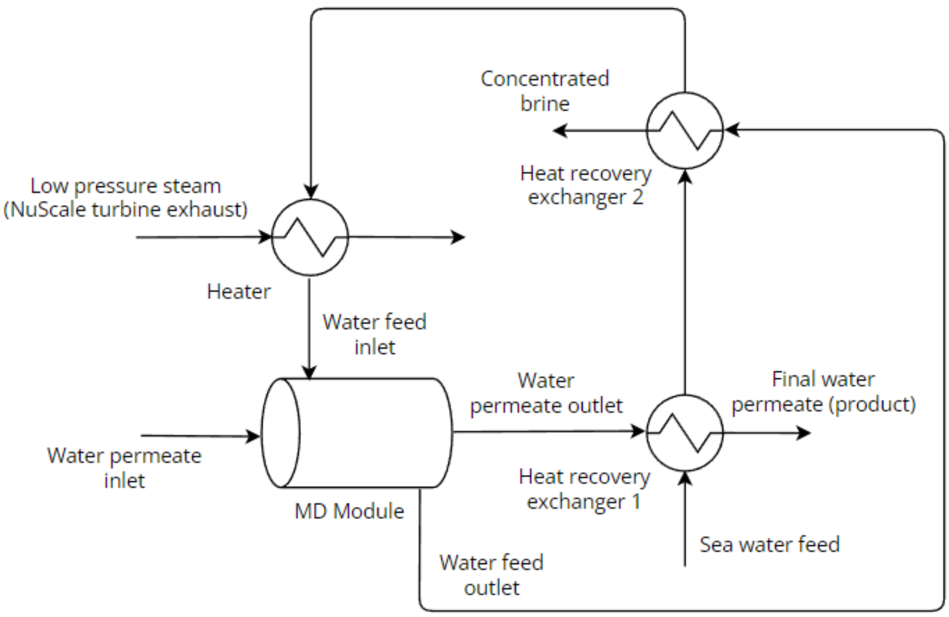

Figure 1. Membrane distillation plant flow diagram with proposed waste heat recovery system.

The partial pressures p_s and p_l, presented in Eq. (1), are calculated by:

$$p_s = (1 - x_s)\alpha_s p_{v,s} \tag{5}$$

$$p_l = (1 - x_l)\alpha_l p_{v,l} \tag{6}$$

where p_v is the vapor pressure and α is the activity coefficient, both calculated at the membrane interface (the subscripts l and s stand for lumen and shell phases). The activity coefficients are calculated by:

$$\alpha_s = 1 - 0.5x_s - 10{x_s}^2 \tag{7}$$

$$\alpha_l = 1 - 0.5x_l - 10{x_l}^2 \tag{8}$$

where x stands for the molar fraction of salt in each phase.

The temperatures at each border of the membrane are computed from Lisboa et al. (2021):

$$T_{m,s} = T_s - (T_s - T_l)\left\{1 + \frac{r_s h_s (T_{m,s} - T_{m,l}) \ln(r_s/r_l)}{k_m (T_{m,s} - T_{m,l}) - j_{w,l} \Delta H_{vap} r_l \ln(r_s/r_l)} + \frac{r_s h_s}{r_l h_l}\right\}^{-1} \tag{9}$$

$$T_{m,l} = T_l + (T_s - T_l)\left\{1 + \frac{r_l h_l (T_{m,s} - T_{m,l}) \ln(r_s/r_l)}{k_m (T_{m,s} - T_{m,l}) - j_{w,l} \Delta H_{vap} r_l \ln(r_s/r_l)} + \frac{r_l h_l}{r_s h_s}\right\}^{-1} \tag{10}$$

where r is the radius, h is the heat transfer coefficient, both with the corresponding subscript, ΔH_{vap} is the vaporization enthalpy and k_m is the membrane thermal conductivity. The subscript m represents the value at the membrane interface.

The countercurrent permeator was modeled as a porous medium and the steady-state energy conservation equation yields (Lisboa et al., 2021):

$$\rho_\gamma c_{p,\gamma} u_\gamma \frac{dT_\gamma}{dz} = -a_\gamma h_\gamma (T_\gamma - T_{m,\gamma}) \tag{11}$$

where γ represents the phase (either lumen or shell) and a is the specific area of the respective phase:

$$a_\gamma = 2N_{fbr} \frac{r_\gamma}{{r_v}^2} \tag{12}$$

and N_{fbr} is the number of fibers in the permeator.

The boundary conditions for Eq. (7) are:

$$T_l(z = 0) = T_{e,l} \tag{13}$$

$$T_s(z = L) = T_{e,s} \tag{14}$$

In order to evaluate the efficiency of the MD process, the gain-output ratio (GOR), which is the ratio between the latent heat carried by the vapor as it is transported through the membrane and the total heat added to the system, was defined as:

$$GOR = \frac{\int_0^L 2\pi N_{fbr} r_l j_{w,l} h_{fg} dz}{\rho_s Q_s c_{p,s}(T_{e,s} - T_{e,l}) - \phi \dot{q}_{hx1} - \phi \dot{q}_{hx2}} \tag{15}$$

where Q stands for the volumetric flow rate, ϕ is the effectiveness of the recovery heat exchangers. $\dot{q}_{hx1}$ and $\dot{q}_{hx2}$ are the maximum heat rates that may be recovered in Heat Exchangers 1 and 2, respectively:

$$\dot{q}_{hx1} = Min(\rho_s Q_s c_{p,s}\,,\ \rho_l Q_l c_{p,l} + 2\pi r_l L N_{fbr} N_p c_{p,l}\, \overline{j_{w,l}})(T_l(L) - T_{e,l}) \tag{16}$$

$$\dot{q}_{hx2} = Min(\rho_s Q_s c_{p,s} - 2\pi r_l L N_{fbr} N_p c_{p,s}\, \overline{j_{w,l}}\,,\ \rho_s Q_s c_{p,s})(T_s(0) - T_{f,hx1}) \tag{17}$$

where N_p is the number of permeator units in parallel, $\overline{j_{w,l}}$ is the mean distillate mass flux, averaged along the permeator length, and $T_{f,hx1}$ is the temperature of the feed solution at the outlet of Heat Exchanger 1, given by:

$$T_{f,hx1} = T_{e,l} + \frac{\phi \dot{q}_{hx1}}{\rho_s Q_s c_{p,s}} \tag{18}$$

Equations (1, 9, 10, 11) were solved iteratively using Wolfram Mathematica v.12.3, assuming the mass and energy imbalances being $\leq 10^{-4}$ within the module as the convergence criteria. The Nusselt number was calculated from:

$$Nu_\gamma = \begin{cases} 4.36 + \dfrac{0.036 \frac{Pe_\gamma}{(L/D_{h,\gamma})}}{1 + 0.0011\left[\frac{Pe}{(L/D_{h,\gamma})}\right]^{0.8}}\,, & Re_\gamma < 2100 \\[2ex] \dfrac{(f_\gamma/8)(Re_\gamma - 1000)Pr_\gamma}{1 + 12.7({Pr_\gamma}^{2/3} - 1)(f_\gamma/8)^{1/2}}\,, & Re_\gamma \geq 2100 \end{cases} \tag{19}$$

where Re is the Reynolds number, calculated as a function of the hydraulic diameter of each phase ($D_{h,\gamma}$), Pe and Pr are the Peclet and Prandtl numbers, respectively, and f is the Darcy friction factor, given by Suga et al. (2022):

$$f_\gamma = \begin{cases} \dfrac{64}{Re_\gamma}\,, & Re_\gamma < 2100 \\[2ex] \dfrac{0.316}{{Re_\gamma}^{0.25}}\,, & Re_\gamma \geq 2100 \end{cases} \tag{20}$$

3. RESULTS

In order to evaluate the distillate production capacity of the desalination plant presented in Fig. 1, which is coupled to the secondary circuit of the NuScale reactor, two variables of the turbine exhaust were obtained from the literature, namely the mass flow rate and vaporization enthalpy (NuScale Power LLC, 2020), as shown in Table 1.

Table 1. Parameters adopted in the simulations of the membrane distillation unit for the NuScale SMR

Parameter	Symbol	Value	Unit
Inner radius of the membrane	r_l	0.49	mm
Thickness of the membrane	δ	235	µm
Inner radius of the shell	r_v	9.5	mm
Conductivity of the polymer	k_p	0.12	W/m·K
Pore diameter	d_p	0.164	µm
Membrane porosity	ε_m	0.9	-
Total pressure in the membrane pore	P	101,325	Pa
Flow rate in the lumen side (one module)	Q_l	0.4	l/s
Flow rate in the shell side (one module)	Q_s	3.0	l/s
Inlet temperature in the lumen side	$T_{e,l}$	24.85	°C
Inlet temperature in the shell side	$T_{e,s}$	40.00	°C
Number of fibers	N_{fbr}	51	-
Length of the permeator	L	450	mm
Mass fraction of salt in the lumen side	w_l	0.000	-
Mass fraction of salt in the shell side	w_s	0.035	-
Total flow rate of permeate solution (entire plant)	$\dot{m}_p$	119	kg/s
Total flow rate of feed solution (entire plant)	$\dot{m}_f$	892.5	kg/s
Turbine exhaust flow rate	$\dot{m}_{steam}$	50.94	kg/s
Turbine exhaust temperature	T_{steam}	41.67	°C
Turbine exhaust vaporization enthalpy	$\Delta H_{vap,steam}$	2,085	kJ/kg
Heat exchanger effectiveness	ϕ	0.9	-

The proposed model was first validated against experimental data (Wang et al., 2008; Yang et al., 2011), shown in Fig. 2. The present model was able to successfully estimate the experimental distillate mass flux achieved for both membrane modules. As it can be seen in Fig. 2a, for higher feed temperatures, such as 70 °C, there is a slight discrepancy and this was expected since the Dusty Gas Model is an isothermal transport model and, thus, less accurate when the transmembrane temperature difference increases.

The parameters adopted in what follows, shown in Table 1, are based on Yang et al. (2011), except for the membrane porosity, which was slightly increased towards optimizing the GOR. The feed temperature at the inlet of the module was set to 40 °C, which is slightly below the temperature of the low-pressure steam (turbine exhaust), before it enters the condenser (41.67 °C). It was estimated for this configuration that the recovered heat from the turbine exhaust enables the production of 1,175.3 m³/day of distilled water. Since this energy would otherwise be wasted, the proposed thermal coupling produced a null power loss in the secondary loop. The assessment with DEEP shows that the same amount of water could be produced by using a traditional technology, such as MED, for the same parameters, at the expense of an electric power loss of 0.41 MWe.

In order to optimize the configuration presented in Table 1, the feed and permeate flow rates were taken as parameters and the resulting effect upon the GOR was analyzed. In Fig. 3, the GOR is presented as a function of the ratio between the feed and the permeate flow rates. As the flow rate ratio decreases, the GOR increases up to a peak value, associated with the ideal flow rate ratio (around 2.1 in this study) and then declines rapidly. As it can be seen, more effective heat recovery provides higher values of GOR. It can also be observed that, for ϕ = 0.9, the GOR peak is approximately three and a half times greater when compared to the system without heat recovery (ϕ = 0). The above described GOR peaking behavior had already been described in the literature (Long et al., 2018). It happens because, as the GOR decreases, the temperature difference across the membrane also decreases, and so does the water flux (GOR numerator), but this effect is counterbalanced by the lower energy demanded for heating the sea water feed (GOR denominator). However, when the flow rate ratio falls below 2.1, the water flux direction across the membrane is inverted, causing the GOR to decline sharply. This happens because, at Q_s/Q_l = 2.1, the temperature difference across the membrane reaches the minimum value necessary for sustaining the water flux from the feed to the permeate. This phenomenon happens due to the smaller activity coefficient in the shell side (Eq. 7) compared to the lumen side (Eq. 8). When Q_s/Q_l < 2.1, the partial pressure in the lumen side (Eq. 6) surpasses the partial pressure in the shell side (Eq. 5), resulting in water flux reversal (Eq.1).

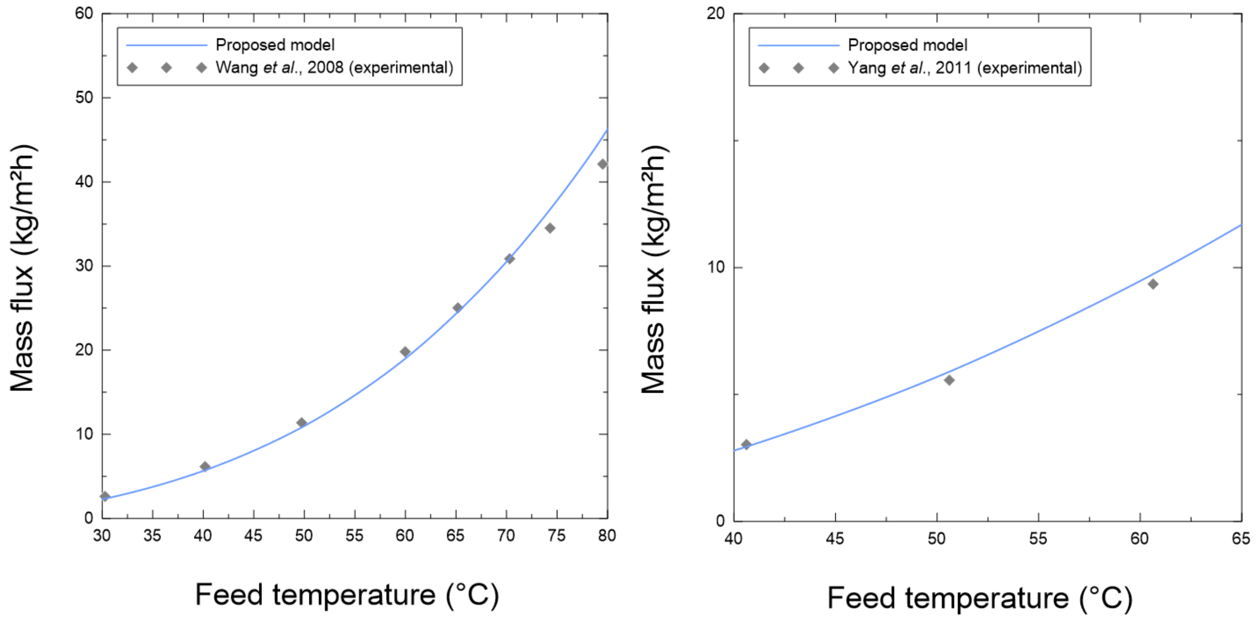

Figure 2. Comparison of theoretical and experimental values of the distillate mass flux as a function of the feed temperature for (a) (Wang et al., 2008) and (b) (Yang et al., 2011).

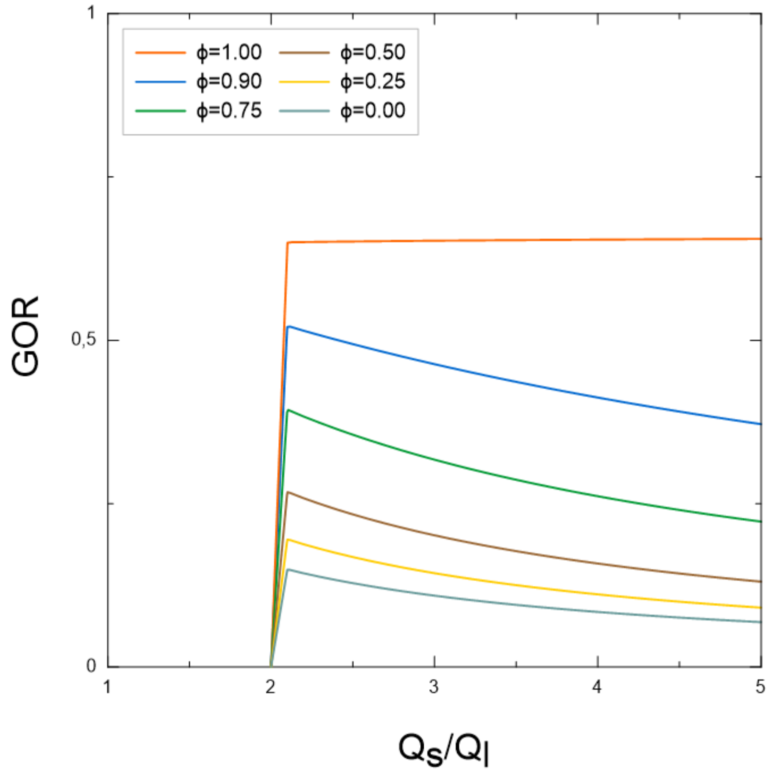

Figure 3. GOR as a function of heat exchanger effectiveness and feed-distillate flow rates ratio, Q_s/Q_l.

Finally, based on the configuration presented in Fig. 1 and Table 1, and optimizing for the ideal flow rate ratio of 2.1, the system is capable of producing a distilled water flux of 2,012.1 m³/day without any reactor power loss, while a MED desalination plant would demand 0.71 MWe from the power plant, for the same distillate production. This value is in accordance with Ingersoll et al. (2014), where linear regression shows that around 0.75 MWe is demanded for producing 2,000 m³/day of water for the NuScale reactor via MED.

4. CONCLUSIONS

The proposed desalination plant is capable of producing around 2,012.1 m³/day of distilled water through direct contact membrane distillation (DCMD), without generating any reactor power loss, whereas the same amount of water produced by MED would demand an electrical power of 0.71 MWe extracted as heat from the reactor secondary system. The heat recovery system played a critical role by increasing the efficiency, measured by the GOR. A system with both heat recovery exchangers operating with an effectiveness of 0.9 presents a GOR three and a half times higher than a system without heat recovery. The ratio between the feed and the permeate flow rates presents an ideal value, which corresponds to a peak in the GOR. In this work, the ideal ratio was around 2.1. As the flow rate ratio decreases from the ideal value, the GOR declines rapidly as the water flux reverses within the module. Future work should explore the liquid and steam extraction stations already available in the NuScale secondary loop design (NuScale Power LLC, 2020), to analyze the available options for increasing the cogeneration of distillate while estimating the inherent electric power generation losses. Also, more efficient membrane distillation configurations shall be analyzed, such as the air gap membrane distillation (AGMD) modules configuration.

5. ACKNOWLEDGEMENTS

The authors are thankful to CAPES (PROCAD/Defesa), CNPq, FAPERJ, Petrogal Brasil, and ANP for the financial support provided.

6. REFERENCES

Alonso, G., Vargas, S., del Valle, E., Ramirez, R., 2012. “Alternatives of seawater desalination using nuclear power”. Nuclear Engineering and Design, Vol. 245, pp. 39–48.

Anjos, E.B., Cárdenas Gómez, A.O., Penaranda Chenche, L.E., Lima, J.A., Naveira-Cotta, C.P., Cotta, R.M., and Lisboa, K.M., 2022, “Enhancing DCMD efficiency for desalination at module scale through dual heat recovery and retentate recirculation”, Proc. of Int. Symp. on Convective Heat and Mass Transfer in Sustainable Energy, CONV-22, Paper # CONV-22-A43, pp.1-8, Izmir Turkey, June 5th-10th.

Cotta, R.M., Pontedeiro, A.C., Sampaio, P.A.B., Jian, S., Aragão de Carvalho, C.A., Carajilescov, P., Naveira Cotta, C.P., Lisboa, K.M., Souza, J.R.B., Freitas, M.A.V., Haguenauer, G.M., 2019. “Pequenos Reatores Modulares (SMRs): Perspectivas em Dessalinização Nuclear”. Conexão Nuclear, ABDAN, Vol. 1, No. 1, p. 19.

Deshmukh, A., Boo, C., Karanikola, V., Lin, S., Straub, A.P., Tong, T., Warsinger, D.M., Elimelech, M., 2018. “Membrane distillation at the water-energy nexus: limits, opportunities, and challenges”. Energy and Environmental Science, Vol. 11, pp. 1177–1196.

Dutta, N., Singh, B., Subbiah, S., Muthukumar, P., 2020. “Performance analysis of a single and multi-staged direct contact membrane distillation module integrated with heat recovery units”. Chemical Engineering Journal Advances, Vol. 4, 100055.

Findley, M., 1967. “Vaporization through porous membranes”. Ind. Eng. Chem. Process Des. Dev., Vol. 6, No. 2, p.226.

IAEA, 2013. “DEEP 5 User Manual.” International Atomic Energy Agency. 10 Jun. 2022 <https://www.iaea.org/sites/default/files/18/08/deep5-manual.pdf (2013)>.

Ingersoll, D.T., Houghton, Z.J., Bromm, R., Desportes, C., 2014. “NuScale small modular reactor for co-generation of electricity and water”. Desalination, Vol. 340, pp. 84–93.

Lisboa, K.M., Souza, J.R.B., Naveira-Cotta, C.P., and Cotta, R.M.,2019. “Heat and mass transfer in hollow-fiber modules for direct contact membrane distillation: Integral transforms solution and parametric analysis”, Int. reverted“Analysis of the membrane effects on the energy efficiency of water desalination in a direct contact membrane distillation (DCMD) system with heat recovery”. Applied Thermal Engineering, Vol. 182, 116063.

Long, R., Lai, X., Liu, Z., Liu, W., 2018. “Direct contact membrane distillation system for waste heat recovery: Modelling and multi-objective optimization”. Energy, Vol. 148, pp. 1060–1068.

Mantero, G., Lomonaco, G., Marotta, R., 2014. “Nuclear desalination: An alternative solution to the water shortage”. Global Journal of Energy Technology Research Updates, Vol. 1, pp. 57–70.

NuScale Power LLC, 2020. Standard Plant Design Certification Application, (Part 2, Tier 2, Chapter 10: Steam and power conversion system).

Sampaio, P.A.B., 2022. “Computational model and simulation of DCMD desalination systems with heat recovery”. Desalination, Vol. 533, 115769.

Suga, Y., Takagi, R., Matsuyama, H., 2022. "Effect of hollow fiber membrane properties and operating conditions on preventing scale precipitation in seawater desalination with vacuum membrane distillation". Desalination, Vol. 527, 115578.

Voutchkov, N., 2018. "Energy use for membrane seawater desalination – current status and trends". Desalination, Vol. 431, pp. 2–14.

Wang, K.Y., Chung, T., Gryta, M., 2008. "Hydrophobic PVDF hollow fiber membranes with narrow pore size distribution and ultra-thin skin for the fresh water production through membrane distillation". Chemical Engineering Science, Vol. 63 (9).

Yang, X., Wang, R., Fane, A. G., 2011. "Novel designs for improving the performance of hollow fiber membrane distillation modules". Journal of Membrane Sciences, Vol. 384 (1-2), pp. 52–62.

7. RESPONSIBILITY NOTICE

The authors are the only responsible for the printed material included in this paper.